JOURNAL OF MATERIALS SCIENCE **37** (2002) 3893 – 3901

Structure and properties of impact modified polyethylene terephthalate

A. AJJI*, N. CHAPLEAU
Industrial Materials Institute, NRC, 75 Boul. de Mortagne, Boucherville, Quebec J4B 6Y4, Canada
E-mail: Abdellah.Ajji@NRC.CA

In this paper, we investigate the orientation behavior of impact modified PET. Core-shell particles, a metallocene polyethylene (mPE) and glycidyl methacrylate modified mPE (gmPE) were blended with PET using single screw extrusion. Morphology, crystallinity, orientation development and mechanical properties of oriented blends were studied following different orientation conditions. It was observed that core-shell impact modifier added to PET does not affect its orientation behavior and that the particles do not deform. Non-reactive mixing with mPE does not affect the orientation developed in PET for the same draw ratio, but the stress levels are affected (higher) due to an earlier crystallization of PET. Reactive blending with gmPE enhances the orientation of PET and the stress levels when orienting are higher than for pure PET, due to an earlier crystallization of PET and strain hardening of mPE being oriented, which indicate a good adhesion at the interface. The elongation at break is affected positively in many cases with the addition of a modifier, particularly gmPE, which is an indication of an improved toughness.

1. Introduction

Orientation of polymers has been used for a long time as means for enhancing polymer properties and found many applications in the areas of fibers, films and bottles. Most of the processes used for those applications involve orientation of the polymers from the melt or rubbery states, such as blow molding and biaxial orientation. Biaxial orientation is even used in some cases to improve the toughness of brittle polymers such as polystyrene [1–3]. However, in some cases, the high orientation levels induced in a polymer may reduce significantly its impact resistance, even for an initially tough material.

For many applications of polymeric materials, mechanical properties are decisive or at least of non-negligible importance. Improvement of toughness of polymers is an important criterion for many applications. Impact toughness or toughness of a material in general reflects the degree of energy absorption from the beginning of mechanical load to final fracture. By incorporating well-defined moderate amounts of dispersed modifier particles with different physical properties in a polymer matrix, its toughness can be improved [4].

Therefore, it is of fundamental importance for the development of polymer systems with improved mechanical properties and toughness, in particular, to understand the relationship between the morphology and deformation behavior of modified polymer systems. Tremendous efforts towards understanding and revealing the mechanisms responsible for improvement of toughness in modified polymer systems have been made in the last two decades. A currently suggested and commonly accepted view on the role of modifier particles is that these inclusions alter the stress state in the material around the particles and induce extensive plastic deformation in the matrix, such as multiple crazing, shear yielding, crazing with shear yielding and rubber particle stretching or tearing and debonding [4]. Because the stress condition around the particles is particularly important in activating matrix plastic deformation, the effects of particle size, interparticle distance and particle cavitation behavior have received considerable attention. PET is usually a tough polymer, but its orientation to high levels somewhat decreases its toughness. It is therefore hoped that its impact modification will allow its energy absorption/toughness to be maintained or enhanced when highly oriented

Sambaru and Jabarin [5] studied the properties and morphology of oriented ternary blends of PET, HDPE and a compatibilizing agent. They studied the effects of orientation temperature, stretch rate, extension ratio, mode of orientation and blend composition. The results showed that blends with compatibilizer (maleic anhydride grafted olefin) show strain hardening upon orientation. The blends with less PET content were difficult to orient. The morphology of the blends showed fibrillar structure, highly oriented in the direction of

*Author to whom all correspondence should be addressed.

stretch. PET underwent stress-induced crystallization upon orientation. The mechanical properties such as modulus and strength showed improvement upon orientation. Simultaneously stretched blends showed better physical properties than sequentially oriented ones [5].

Carté and Moet [6] studied the morphological origin of super toughness in PET/PE blends. The compatibilization strategy used to achieve high toughness was the addition of maleic anhydride functionalized styrene-ethylene-buthylene-styrene (MA-g-SEBS) block copolymer. Addition of 20% copolymer was found to produce an intricate multidomain morphology in which the two major components (50% PE and 50% PET) and the compatibilizer coexist on a hierarchical order. A portion of PET was dispersed as interconnected rodlike domains oriented along the injection direction. The rest of PET and PE constituted beadlike nano domains that served as the matrix. The blend at all levels responded to deformation in a cooperative fashion giving rise to super tough material that has an elongation to break of 600% in comparison to 90% for PET and 300% for HDPE [6].

Tanrattanakul *et al.* [7] studied the effect of elastomer functionality on toughened PET by addition of 5% SEBS grafted with 0 to 4.5 wt% maleic anhydride onto the ethylene-butylene midblock. Graft copolymer formed by reaction of PET hydroxyl end groups with the anhydride *in situ* was thought to act as an emulsifier to decrease interfacial tension and promote adhesion. All the elastomers increased the melt viscosity of PET, however, the amount and functionality of the elastomer did not have a large effect on blend rheology. In contrast, particle size was strongly dependent on the elastomer functionality: the higher the functionality, the smaller the particle size and the narrower the particle size distribution. Furthermore, elastomer content had less effect on the particle size as the functionality increased, and the tendency toward increasing particle size with increasing elastomer content diminished. These trends were attributed to an increase in the degree of grafting on the in situ graft copolymer. Particles of functionalized SEBS were primarily spherical in injection molded blends in contrast to the highly elongated particles of unfunctionalized SEBS. In un-notched tensile tests, blending PET with any SEBS enhanced the stability of the propagation neck. Notched tensile tests differentiated among the blends in terms of their toughness. The least effective elastomer was the unfunctionalized SEBS. The most effective was the SEBS with only 1% anhydride. The decrease in toughness with increasing functionality was attributed to decreasing particle size.

In this paper, we investigate the effect of drawing and interfacial modification of impact modified PET on the blends morphology, adhesion between the phases, orientation and tensile mechanical properties, particularly the elongation at break.

2. Experimental details

2.1. Blends preparation and drawing

Bottle grade polyethylene terephthalate copolyester (PET) of undisclosed composition was used (Shell Cleartuf 8006). Different impact modifiers were used with PET: core-shell particles having a hard core and soft shell made from partially cross-linked acrylic-beads 330 nm in diameter (Rohm & Haas Paraloid EXL-3330), a metallocene polyethylene (mPE) and a grafted mPE (gmPE). The mPE was Engage 8200 with a melt flow index of 5, a density of 0.87 and contained 25% octene. The gmPE was produced in house by grafting 0.48% by weight of glycidyl methacrylate (GMA) to the metallocene. Blending and sheet extrusion were performed on a Brabender 3/4" single screw extruder equipped with a pin screw to minimize degradation. A temperature of 260°C and rotating speed of 50 RPM were used. A flat die (1 mm opening) followed by a calendering unit with rolls chilled at room temperature were used in producing 0.4 mm thick sheets.

The tensile drawing was performed on an Instron tensile tester at 90°C (above the glass transition of PET) and 15 cm/min drawing rate. Quenching of the samples was performed by opening the door of the oven at the end of the drawing experiment. The draw ratio applied ranged from 1 to 5.

2.2. Characterization of the structure and performance

2.2.1. Microscopy

Scanning Electron Microscopy was performed on fractured surfaces in liquid nitrogen (longitudinal and transverse directions) in a JOEL Model JSM-T220 microscope on Au-Pd sputter coated specimen. In some cases, microtomed surfaces were also examined.

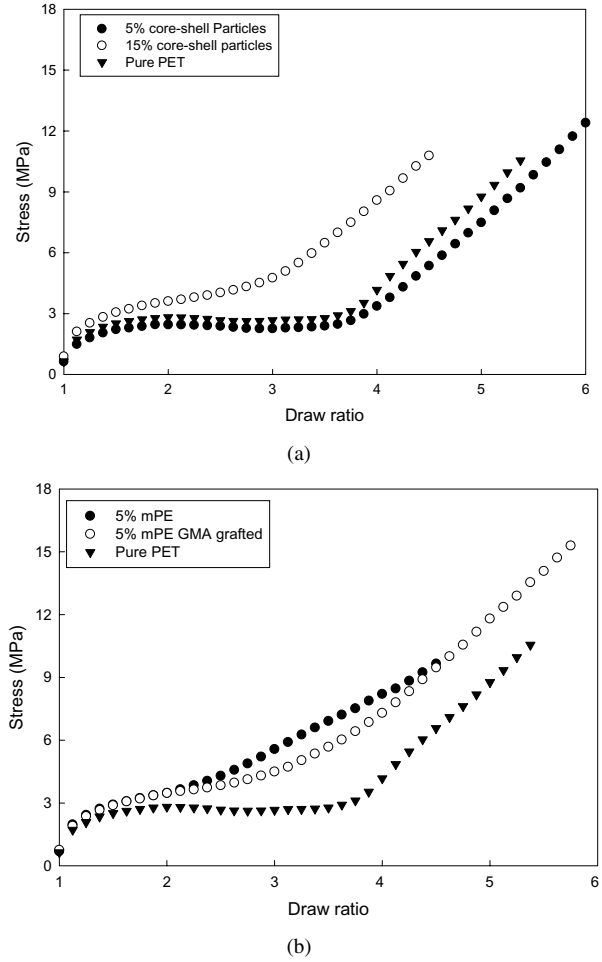

Figure 1 (a) Stress-strain curves for PET and blends with 5 and 15 wt% core-shell particles. (b) Stress-strain curves for PET and blends with 5 wt% mPE and 5 wt% gmPE.

2.2.2. Thermal analysis

Measurements have been done using a Perkin-Elmer DSC-7 instrument. The crystallinity of the PET samples was determined using the area under melting and crystallization peaks, assuming a heat of fusion for fully crystalline PET as $\Delta H_m^\circ = 140$ J/g [8]. The heating rate used for the scans was 20°C/min.

2.2.3. Spectrographic birefringence

Birefringence measurements were made using a multiwavelength light source. The birefringence value, corresponding to a wavelength of 589.6 nm was calculated by fitting the measured transmitted intensity versus wavelength curve. More details on this technique can be found elsewhere [9, 10].

2.2.4. Infra red spectroscopy

Polarized FTIR spectra were taken on selected drawn samples of PET, mPE and gmPE modified PET in the parallel and perpendicular polarization to determine the orientation of the PET and blends.

2.2.5. Mechanical properties

Modulus, strength and elongation at break (related to the energy absorbed by the material or its toughness) were determined using a tensile testing machine operated at a crosshead speed of 10 cm/min at room temperature (20 mm gauge length).

3. Results and discussion

Fig. 1a shows the drawing behavior at 90°C of PET modified by addition of core-shell particles in terms of engineering stress as a function of draw ratio. Both the neat PET and the blend with 5% core-shell particles show a similar behavior and the maximum draw ratio is little affected. At 15%, the modified PET blend shows an early strain hardening and a reduced maximum draw ratio. Such accelerated strain hardening might be related to the nucleating effect of the core-shell particles and the reduced PET volume fraction, which increase the real stress in the PET phase. These hypotheses are supported by microscopic observations showing no adhesion at the PET-particles interfaces with no deformation of the acrylic core-shell particles and by the

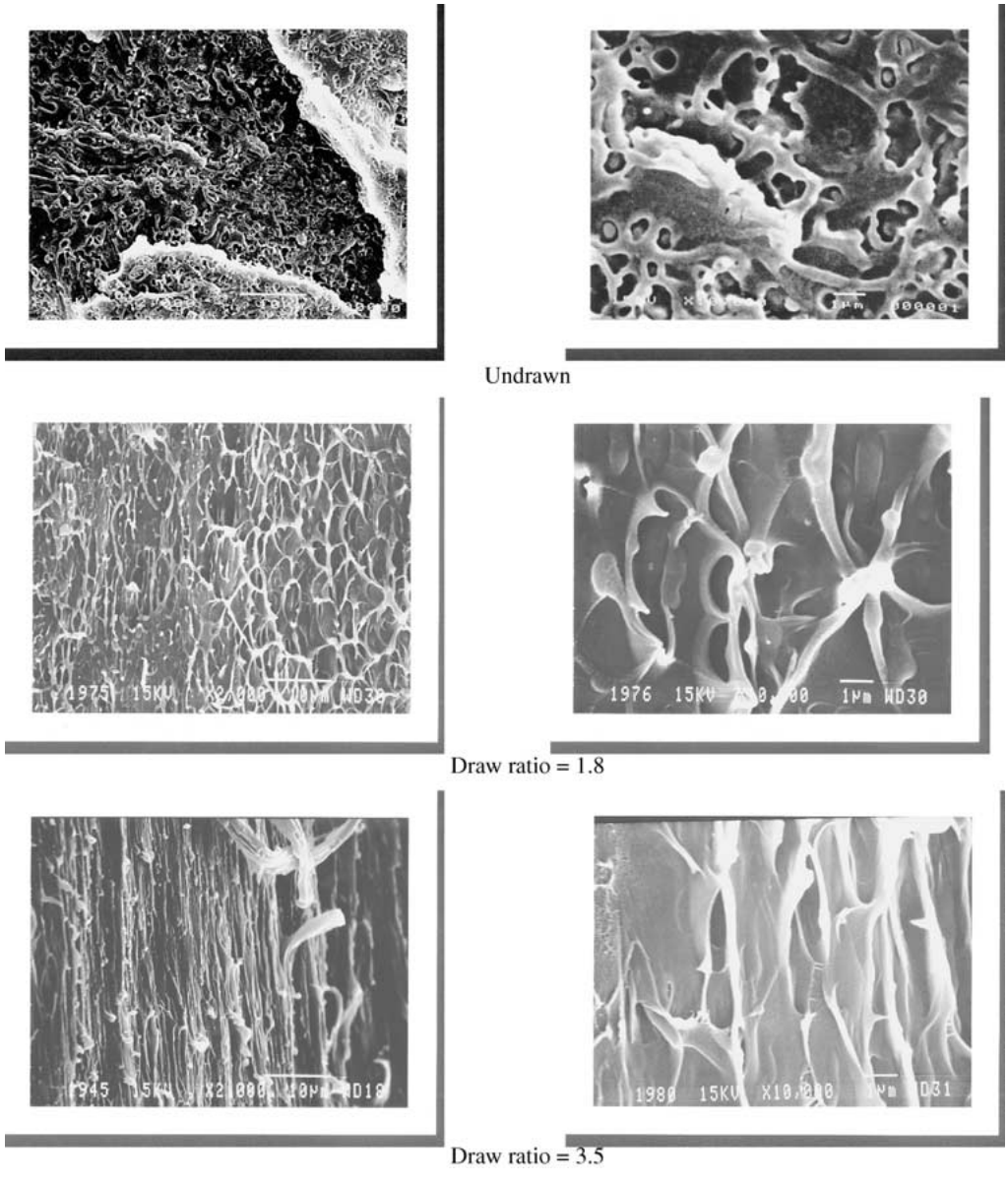

Figure 2 SEM micrographs of cryogenically fractured surfaces of PET blends with 5 wt% core-shell particles drawn to different draw ratios.

results of crystallinity measurements that will be discussed later.

Fig. 1b shows the same results but for the mPE and gmPE modified PET to the 5 wt% level. The mPE blend shows much lower drawability with an earlier strain hardening. The poor adhesion between the two phases creates rupture sites, which limits the maximum draw ratio of the blend. In contrast, the gmPE blend shows an improved drawability and the gmPE dispersed particles acts as a nucleating agent. Since a good adhesion is expected, as will be discussed later, both phases elongate upon deformation and no local voids are formed that may initiate premature rupture.

Figs 2 to 7 show micrographs of the different undrawn and drawn blends to different draw ratios. Figs 2 and 3 show the morphology of blends with 5 and 15% core shell particles respectively obtained on cryogenically fractured surfaces. It is clear that no adhesion is developed with the PET matrix and elongated PET strands are clearly visible due to debonding at the interface and drawing. Some aggregation of the particles can also be observed in the micrographs. Figs 4 and 5 show the morphology of the blends containing 5% mPE and gmPE respectively, obtained from cryogenically fractured surfaces. The mPE blend shows dispersed phase domains of 5–10 μm, slightly elongated for the undrawn blend, certainly due to the extrusion process. Upon drawing to draw ratios from 1.5 to 4.2, it is seen that the mPE, domains elongate as well as the voids created due to debonding. For the gmPE blends, the dispersed phase size is much lower, in the range of 1–2 μm, and is not deformed before drawing. Very little debonding is observed upon drawing and gmPE domains are well elongated.

Micrographs of microtomed surfaces were also observed for the blends and are shown on Fig. 6a and b for core-shell particles blends and a draw ratio of about 3.4. It is even more obvious from these micrographs that there is no adhesion and that the core shell particles just become detached upon drawing and the cavities

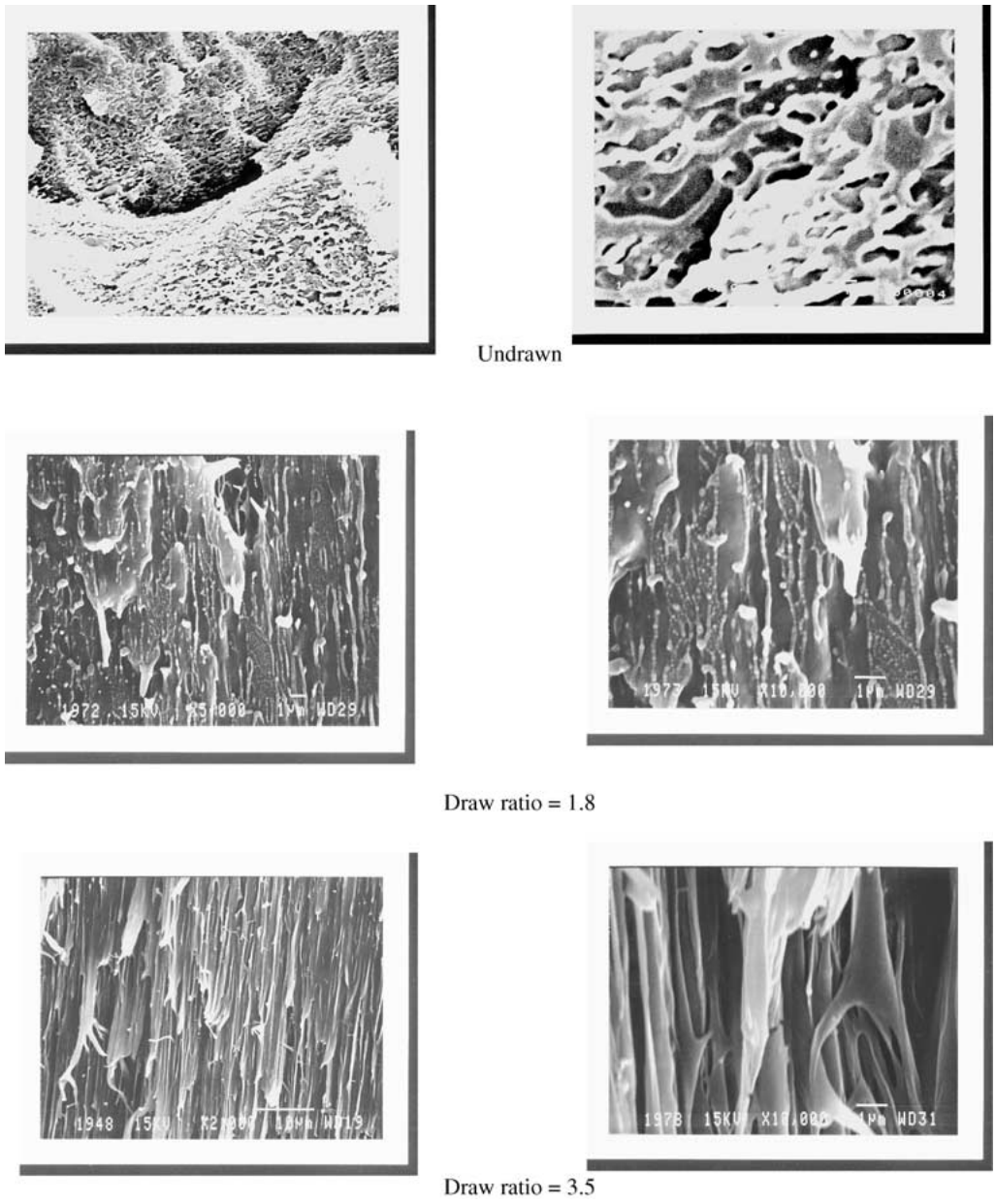

Figure 3 SEM micrographs of cryogenically fractured surfaces of PET blends with 15 wt% core-shell particles drawn to different draw ratios.

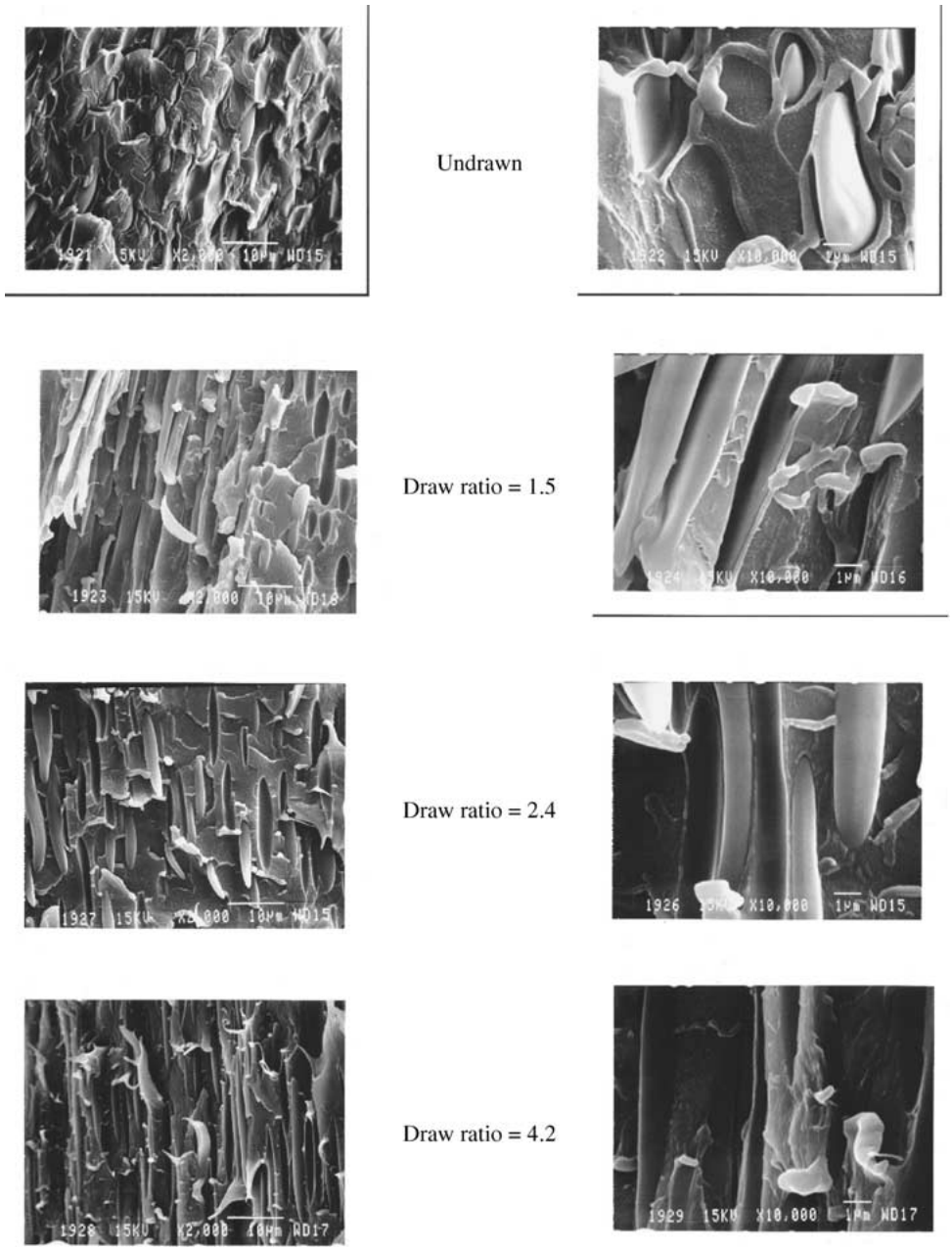

Figure 4 SEM micrographs of cryogenically fractured surfaces of PET blends with 5 wt% mPE drawn to different draw ratios.

are elongated. Similar micrographs for mPE and gmPE blends are presented Fig. 7a and b. Further evidence of the observations mentioned above can be observed on these microtomed surfaces, where the difference in size and adhesion of mPE and gmPE domains is clearly evidenced for the draw ratio of 4.2.

Fig. 8 shows the crystallinity measurement results as a function of draw ratio obtained on PET and blends. The maximum crystalline content is higher for pure PET, which is expected because of a reduced weight fraction of PET in the blends and the absence of any additive. All the blends show a lower crystallinity for high draw ratios and an earlier crystallization due to a nucleating effect, as mentioned above.

All the blends were transparent enough for light to allow birefringence measurement in transmission. The results of these measurements as a function of draw ratio are presented in Fig. 9a and b for blends with core-shell particles and with mPE, respectively. For core-shell blends, the birefringence of PET and blends are mainly the same, since there is no adhesion and the particles are not expected to contribute to the overall birefringence. This indicates mainly that the orientation of the PET phase is the same, as clearly observed in Fig. 9a. For the blend with mPE, a similar result is also obtained with the same conclusion as no adhesion is expected in this case also (Fig. 9b). In contrast, blends with gmPE show a higher birefringence, particularly at draw ratios above 3, for which a crystalline morphology is present. This result concurs with previous indications of strong adhesion and orientation of the disperse phase. At a draw ratio around 4.5 for example, about 40% increase in birefringence is observed. This is about 0.040 in terms of birefringence, close to the maximum birefringence of 0.065 for PE, which is possible since PE reaches its maximum birefringence at draw ratios around 4–5.

In order to confirm this higher orientation of the PE phase in the blend when using grafted mPE, polarized infrared spectra measurements were performed on PET

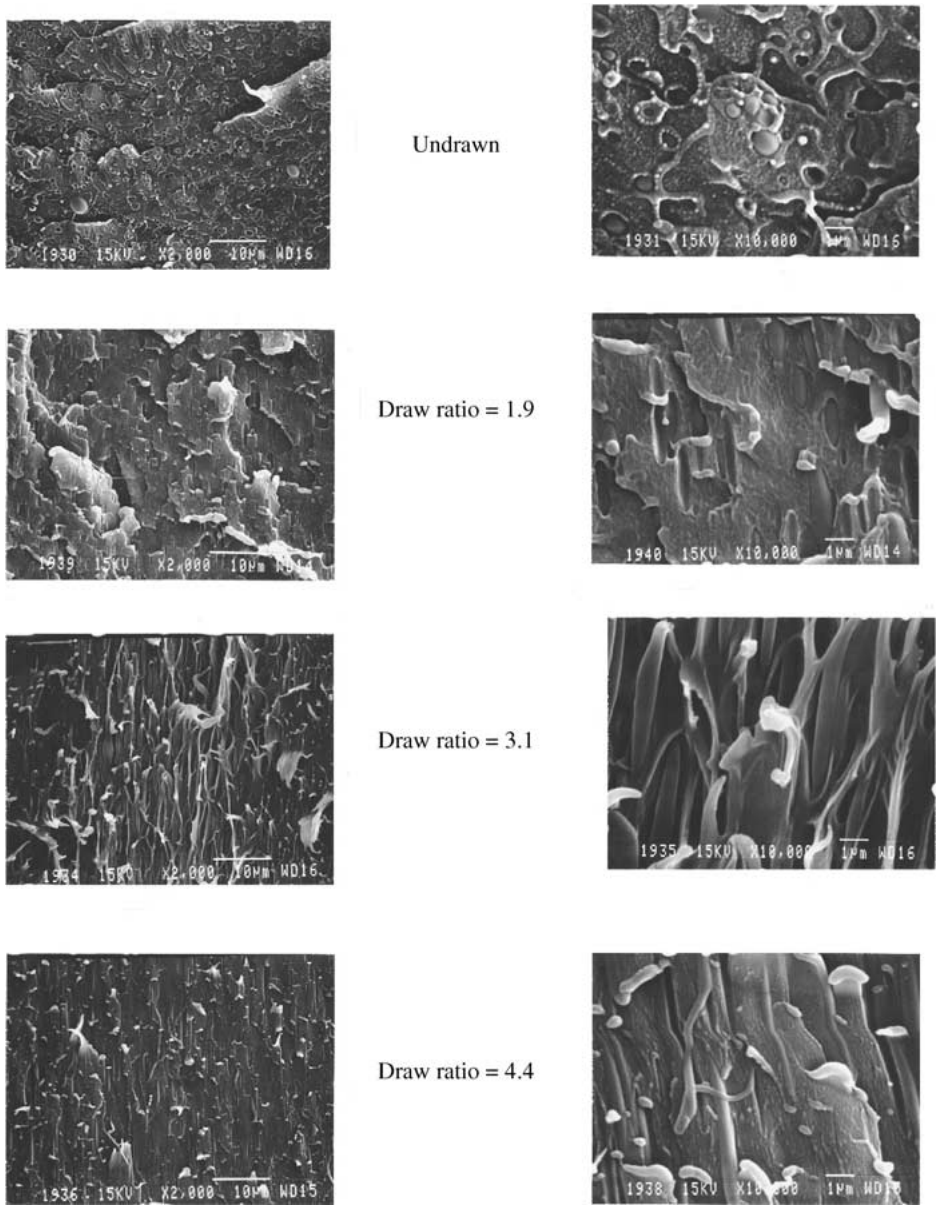

Figure 5 SEM micrographs of cryogenically fractured surfaces of PET blends with 5 wt% gmPE drawn to different draw ratios.

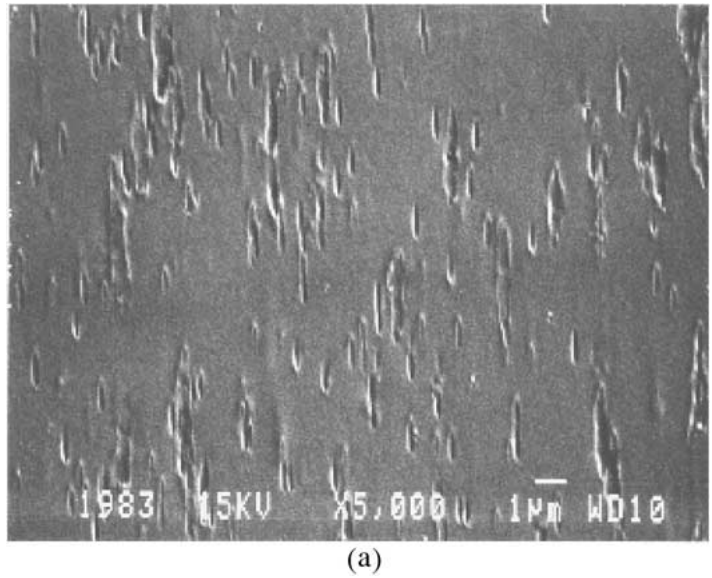

(a)

Figure 6 SEM micrographs of microtomed surfaces of (a) 5 wt% core-shell particles modified PET and (b) 15 wt% core-shell particles modified PET, both drawn to a draw ratio of 3.5. (*Continued.*)

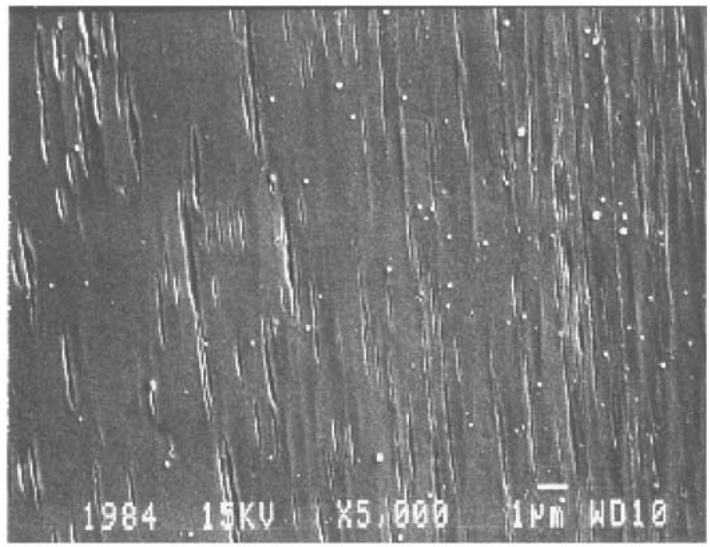

(b)

Figure 6 (*Continued*).

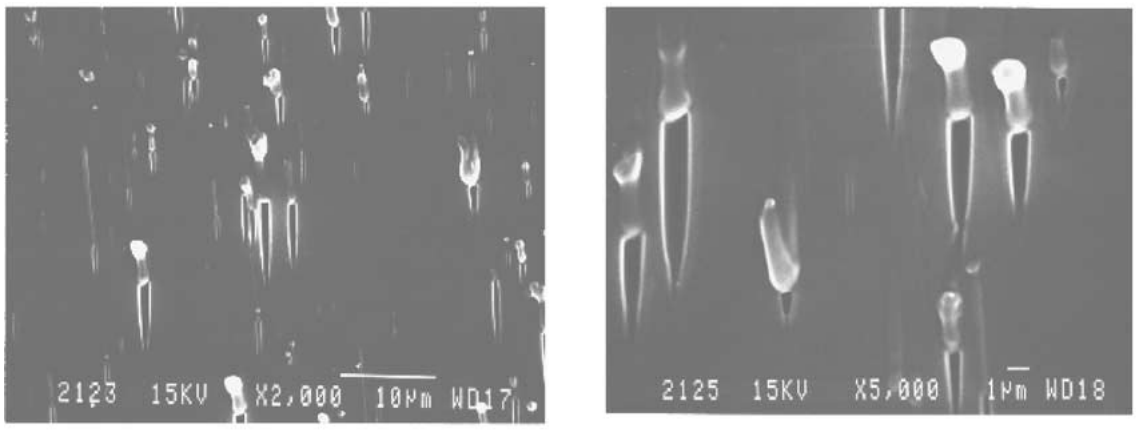

(a) 5% mPE, draw ratio 4.2

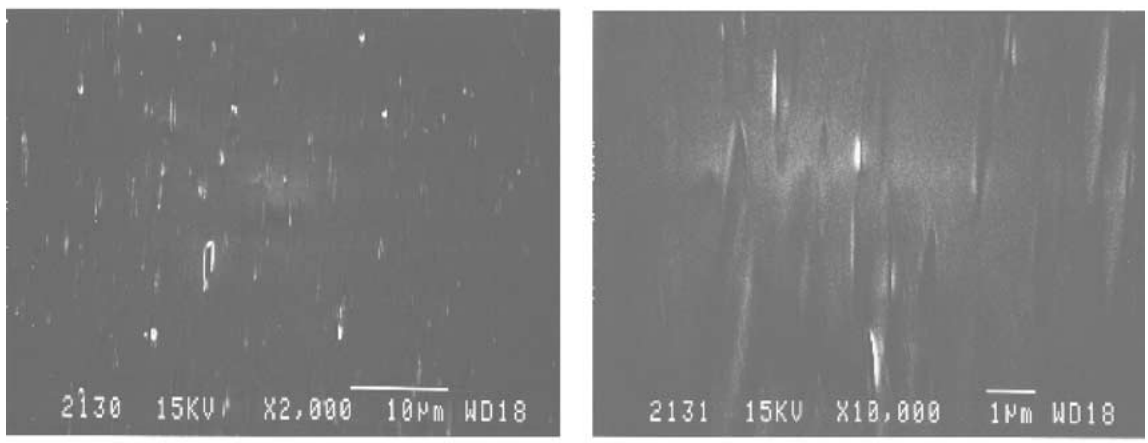

(b) 5% gmPE, draw ratio = 4.2

Figure 7 SEM micrographs of microtomed surfaces of (a) 5 wt% mPE modified PET and (b) 5 wt% gmPE modified PET, both drawn to a draw ratio of 4.2.

and blends with mPE and gmPE oriented to a draw ratio around 3.5. Subtraction of the spectra in the parallel and perpendicular polarizations will indicate the dichroic vibrations and the area under these vibrations is indicative of the level of orientation. Fig. 10 shows the results obtained in the wavenumber range of 2800–3200 cm^{-1}. There is a vibration around 2850 cm^{-1} that is due to the mPE phase and which does not overlap on any PET vibration. It is clearly observed that the area under this peak is much higher for the gmPE blend than it is for the mPE one. It is also clear that the mPE phase is oriented in the ungrafted mPE blend. This is a clear evidence of

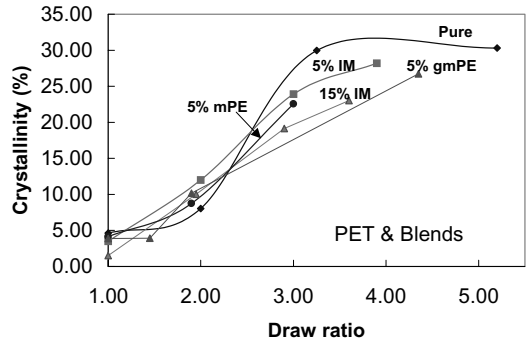

Figure 8 Crystallinity as a function of draw ratio for PET and blends as indicated.

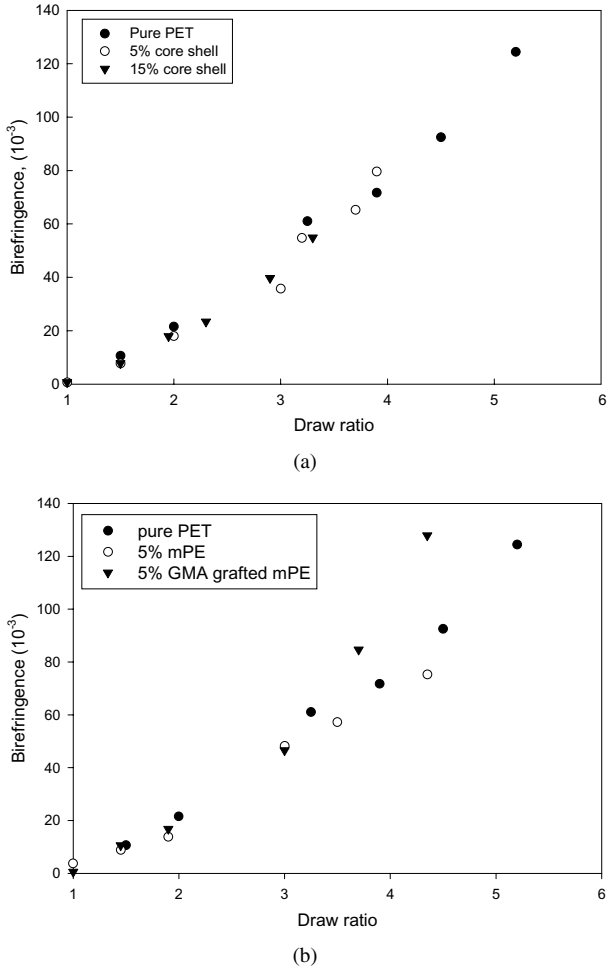

Figure 9 (a) Birefringence of PET and core-shell particles blends as a function of draw ratio. (b) Birefringence of PET, mPE and gmPE blends as a function of draw ratio.

a much higher adhesion between PET and gmPE due to the reaction with grafted groups and confirms all the observations and speculations stated above.

Figs 11 to 13 show the results obtained on the mechanical properties of the different blends in tension in terms of modulus, strength and elongation at break respectively as a function of draw ratio. A large scatter in the data is observed and the modulus and strength remain essentially the same for all the blends. The standard deviations bars are indicated on the figures for each case. The modulus and strength increase significantly around a draw ratio of 2.5 due to the crystalline structure developed. A close look at the elongation at break show that for the blend with gmPE, higher elongations,

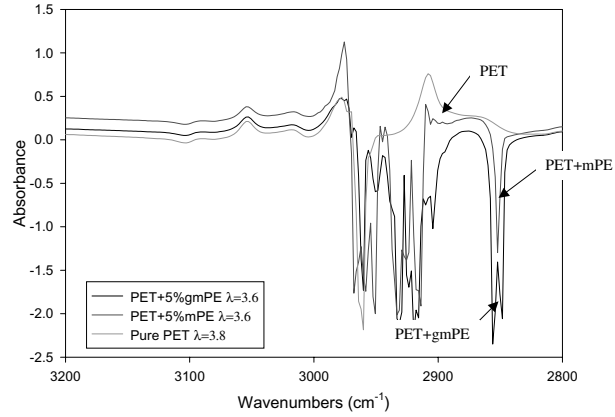

Figure 10 Infrared difference spectra between parallel and perpendicular polarizations for PET, mPE and gmPE blends drawn to a draw ratio of about 3.6.

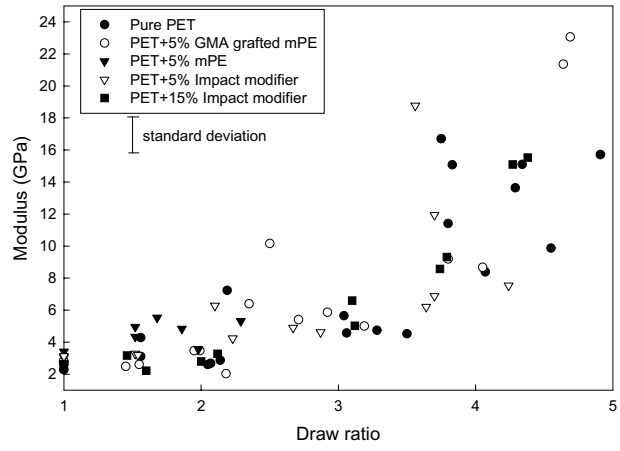

Figure 11 Tensile modulus as a function of draw ratio at room temperature for PET and blends.

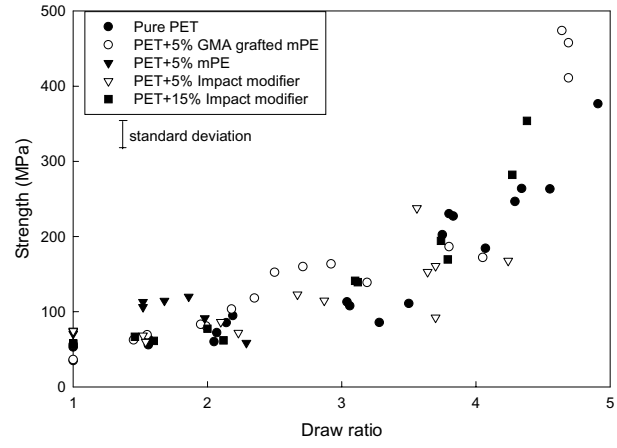

Figure 12 Tensile strength as a function of draw ratio at room temperature for PET and blends.

compared to pure PET and the other blends, are obtained up to a draw ratio of 3. This is an indication of an improvement in impact toughness (energy absorption) of these blends, since it is related to the area under the stress-strain curve.

From all the above-discussed results, it is clear that the inclusions alter the stress state in the material around the particles and induce extensive plastic deformation in the matrix. These include multiple crazing, shear yielding, crazing with shear yielding and rubber particle stretching or tearing and debonding [4] as well

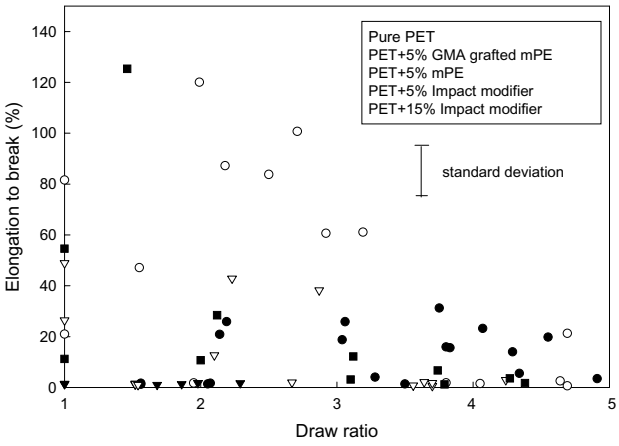

Figure 13 Elongation at break as a function of draw ratio at room temperature for PET and blends.

as deformation of the particles in the case of high adhesion. The Graft copolymer formed by reaction of PET hydroxyl end groups with the anhydride *in situ* is thought to act as an emulsifier to decrease interfacial tension and promote adhesion, which is clear from the large deformation observed from microscopy and orientation from FTIR for the gmPE blends. The use of modifiers such as gmPE in PET enhances then the adhesion, stretchability and toughness of the blends.

4. Conclusions

In conclusion, it was observed that core-shell impact modifiers added to PET do not affect its orientation behavior and that the particles do not deform. Non-reactive mixing of metallocene PE does not affect the orientation developed in PET for the same draw ratio, but the stress levels are affected due to an earlier crystallization of PET. Reactive blending with GMA-grafted mPE enhances the orientation of PET (increased birefringence for the same draw ratio) and the stress levels when orienting are higher than for pure PET due to an earlier crystallization of PET and strain hardening of mPE being oriented, which indicate a good adhesion at the interface. Finally, the elongation at break for the oriented blends with GMA-grafted mPE is improved.

References

1. R. YAN, A. AJJI and D. M. SHINOZAKI, *Polym. Eng. Sci.* **41** (2001) 618.
2. *Idem.*, *Polymer* **41** (2000) 1077.
3. R. YAN, A. AJJI, D. M. SHINOZAKI and M. M. DUMOULIN, *J. Mater. Sci.* **34** (1999) 2335.
4. C. B. BUCKNALL, in "Toughened Plastics" (Applied Science, London, 1977).
5. P. SAMBARU and S. A. JABARIN, *Polym. Eng. Sci.* **33** (1993) 827.
6. T. L. CARTÉ and A. MOET, *J. Appl. Polym. Sci.* **48** (1993) 611.
7. V. TANRATTANAKUL, A. HILTNER, E. BAER, W. G. PERKINS, F.L. MASSEY and A. MOET, *Polymer* **38** (1997) 4117.
8. B. WUNDERLICH, *Polym. Eng. Sci.* **18** (1978) 431.
9. A. AJJI, J. GUÉVREMONT, R. G. MATTHEWS and M. M. DUMOULIN, SPE ANTEC'98 Proceedings (1998) p. 1588.
10. A. AJJI and J. GUÉVREMONT, U.S. Patent no. 5,864,403 (1999).

Received 29 August 2001
and accepted 6 May 2002